

## Singular structure in the density of levels of simple metals

N. W. Ashcroft

*Laboratory of Atomic and Solid State Physics, Cornell University, Ithaca, New York 14853*

(Received 25 September 1978)

Local pseudopotential components  $V_{\vec{k}}$  are available in many of the simpler metals, either from measurement or by direct computation. Given these it is shown that by invoking generally no more than a three-band model throughout the zone, a straightforward method is available for obtaining the principal features of the density of levels. Certain of these features, those recognizably due to the form of the bands near zone planes, for example, have their counterparts at zone-plane intersections and these are shown to arise from Van Hove singularities on otherwise nearly-free-electron band structures. In the case of aluminum, the example used to illustrate the method, it is shown that significant single-particle band-structure effects are present in the density of levels at the Fermi energy.

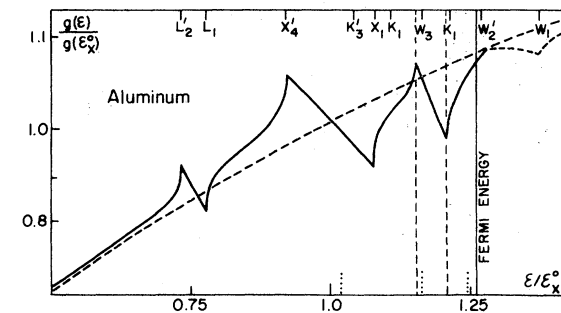
## I. INTRODUCTION

Figure 1(a) shows a portion of a calculated density of levels in aluminum. Some of the rather noticeable structure displayed there is readily identified with band extrema associated with the levels  $L_2'$ ,  $L_1$ , and  $X_4'$ ,  $X_1$ , which in turn are connected with the centers of the  $\{111\}$  and  $\{200\}$  sets of planes of the first Brillouin zone [Fig. 1(b)]. The singular features may be referred to as zone-face structure. Equally apparent, however, is some sharp structure somewhat reminiscent of

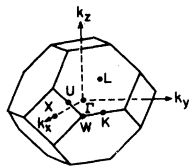
this zone-face structure, located near but not quite at the levels belonging to symmetry points  $K$  (or  $U$ ) and  $W$ . The origin and magnitude of this structure, which may be termed zone-edge structure, is a major concern of what follows. In addition there are other singular features in the density of levels of a very much weaker character than those displayed in Fig. 1(a). These occur as a consequence of the touching of bands. A secondary objective of this paper is to examine the nature of these minor singular features, to locate them in energy, and to estimate the corrections they may make to Fig. 1(a) (which omits them).

The overall structure just described is not specific to aluminum but is generally to be found in the class of nearly-free-electron-like metals although not necessarily in the order presented. One of the purposes of this paper is to show that the singular structure in the density of levels can be accounted for by a straightforward analysis restricted to certain portions of the band structure. With the exception of the minor band contact features the major singular points in the density of levels are rather simply related to the principal pseudopotential components  $\{V_{\vec{k}}\}$  used to interpolate the band structures. In many cases the important  $V_{\vec{k}}$  can be extracted from an analysis of measured Fermi surfaces.<sup>1</sup> In others, particularly the simple polyvalent metals, they may be obtained quite directly, at least within the local-pseudopotential approximation, by locating the positions of the major interband absorption edges in the optical-response function.<sup>2</sup> Nonlocal contributions are not always small, but for the purposes of illustrating the methods to be used here, those manifestations of nonlocal effects that cannot be subsumed within appropriate effective masses<sup>3</sup> will be neglected.

Sections II-IV are devoted to a description of the methods required to calculate in terms of the  $V_{\vec{k}}$  the singular contributions of the density of levels.



(a)



(b)

FIG. 1(a) Singular structure in the calculated density of levels of  $g(\mathcal{E})$  of aluminum arising from ordinary critical points in the band structure. Small vertical dotted lines indicate the location of structure arising at energies  $\mathcal{E}$  corresponding to higher critical points (see Sec. IV). The energy  $\mathcal{E}_x^0$  is the free-electron energy at  $k = k_x = 2\pi/a$ . (b) First Brillouin zone of the fcc structure.

Underlying the methods is an application of perturbation theory in conjunction with certain general results of Van Hove<sup>4</sup> and Phillips<sup>5</sup> pertaining to the nature of critical points in the excitation spectra of periodic systems.<sup>6</sup> As will become evident, it is generally sufficient to consider the properties of, at most, a three-band model. Results are given, by way of illustration, for aluminum which is taken as a representative nearly-free-electron system.

It is assumed throughout that the independent-particle picture or at least a quasiparticle picture is an acceptable starting point for the analysis. The polyvalent metals (including equivalent polyvalent intermetallics) are therefore particularly suited to this analysis since the important structure falls near the Fermi energy where the quasiparticle picture is most likely to be valid.

## II. DENSITY OF LEVELS: ZONE-FACE STRUCTURE

Figure 2 shows sufficient of an aluminum band structure<sup>7</sup> to display the regions responsible for the details in the density of levels noted in Fig. 1(a). In the neighborhood of a single zone plane (and far from the intersections of such planes) it is customary to consider a standard  $(2 \times 2)$  secular equation. For the present purposes however, the three-band problem<sup>8</sup>

$$\begin{vmatrix} T_0(\vec{k}) & U_{\vec{K}} & U_{\vec{K}} \\ U_{\vec{K}} & T_{\vec{K}}(\vec{k}) & 0 \\ U_{\vec{K}} & 0 & T_{-\vec{K}}(\vec{k}) \end{vmatrix} = 0, \quad (1)$$

has a useful symmetry which aids in determining the correction to the free-electron density of levels. Here

$$T_{\vec{K}}(\vec{k}) = (\hbar^2/2m^*)(\vec{k} - \vec{K})^2 - \mathcal{E},$$

where  $m^*$  is an effective mass, and  $\vec{K}$  a reciprocal-lattice vector for the structure under consideration. For low-order secular equations the  $U_{\vec{K}}$  are to be regarded as *folded* Fourier components<sup>9</sup> of the pseudopotential as constructed from the  $V_{\vec{K}}$ .

From (1) it is evident that the three bands must have the form

$$\mathcal{E}_m(\vec{k}) = (\hbar^2/2m^*)k_{\parallel}^2 + H_m(k_{\parallel}), \quad m = 1, 2, 3, \quad (2)$$

where  $H_m(k_{\parallel})$  is entirely a function of  $k_{\parallel}$ , the component of  $\vec{k}$  parallel to  $\vec{K}$  ( $k_{\perp}$  being the perpendicular component). To obtain the contribution  $G_m(\mathcal{E})$  to the density of levels from the  $m$ th band at energy  $\mathcal{E}$ , we start from<sup>10</sup>

$$G_m(\mathcal{E}) = \frac{\Omega}{4\pi^3} \int_{S_m(\mathcal{E})} \frac{dS_m}{|\nabla_{\vec{k}} \mathcal{E}_m(\vec{k})|} \Theta(\mathcal{E} - \mathcal{E}_m(\vec{k})), \quad (3)$$

where  $\Omega$  is the total volume (containing  $N$  electrons) and  $S_m(\mathcal{E})$  is the branch in the  $m$ th band of

the surface of constant energy  $\mathcal{E}$ . From (2) and (3) we find

$$G_m(\mathcal{E}) = (3N/2\mathcal{E}_F^0) k_{\parallel}^{(m)}(\mathcal{E})/k_F = G^0(\mathcal{E}_X^0) [k_{\parallel}^{(m)}(\mathcal{E})/k_X], \quad (4)$$

where  $G^0(\mathcal{E}_X^0)$  is the free-electron density of levels at  $\mathcal{E} = \mathcal{E}_X^0$ , and in turn  $\mathcal{E}_X^0$  is the free-electron energy at  $k = k_X = 2\pi/a$ . In (4)  $\mathcal{E}_F^0$  is the free-electron Fermi energy, and  $k_{\parallel}^{(m)}(\mathcal{E})$  is the solution for fixed  $\mathcal{E} = \mathcal{E}_m(\vec{k})$  of (2) with  $k_{\perp} = 0$ . If we define,

$$g_m(\mathcal{E}) = G_m(\mathcal{E})/G^0(\mathcal{E}_X^0), \quad e_m = \mathcal{E}_m/\mathcal{E}_X^0,$$

and

$$\vec{p} = \vec{k}/(2\pi/a),$$

then

$$e_m(\vec{p}) = p_{\parallel}^2 + h_m(p_{\parallel}) \quad [h_m(p_{\parallel}) = H_m/\mathcal{E}_X^0]$$

and

$$g_m(e) = p_{m,\parallel}(e). \quad (5)$$

We proceed to find for each symmetric-zone-plane pair the contribution from (5) that is in excess of  $g(e) = \sqrt{e}$ , the result for  $U_{\vec{K}} = 0$ . This is most easily achieved by rewriting the secular Eq. (1) in dimensionless variables

$$\epsilon = (2\pi/aK)^2(e - p_{\parallel}^2), \quad (6a)$$

$$u = (2\pi/aK)^2(U_{\vec{K}}/\mathcal{E}_X^0), \quad (6b)$$

$$q = k_{\parallel}/K = (2\pi/aK)p_{\parallel}, \quad (6c)$$

and

$$\epsilon = q^2 - y + \frac{2}{3}. \quad (7)$$

Then after a little manipulation Eq. (1) can be cast in either of two forms. First as

$$y^3 - y(4q^2 + 2u^2 + \frac{1}{3}) = -\frac{2}{3}(4q^2 - u^2 - \frac{1}{9}), \quad (8)$$

in which the coefficients of this standard cubic form explicitly depend on reduced wave vector  $q$ . Using (7) the solutions to (8) therefore give the band structure:

$$\epsilon_m(q) = q^2 + \frac{2}{3} - (2/\sqrt{3})(4q^2 + 2u^2 + \frac{1}{3})^{1/2} \times \cos\left\{\frac{1}{3} \arccos\left[\frac{\sqrt{3}(4q^2 - u^2 - \frac{1}{9})}{(4q^2 + 2u^2 + \frac{1}{3})^{3/2}}\right]\right\}, \quad (9)$$

with  $m = 1, 2,$  or  $3$  according to the branch of the arccosine chosen (see Appendix A). For the choice  $u = 0.05$  these bands are plotted in Fig. 3. They have the expected extrema, the band gap at  $q = \frac{1}{2}$  being  $|2u| + O(u^2)$ , for example.

The density of levels, in which we are primarily interested, follows from writing (1) in its second form:

$$y^3 - y(4\epsilon + 2u^2 + \frac{1}{3}) = \frac{2}{3}(4\epsilon + 5u^2 - \frac{1}{9}), \quad (10)$$

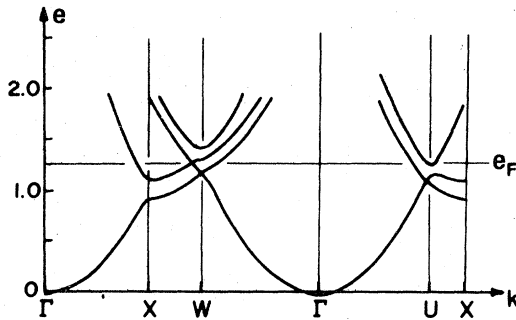


FIG. 2. Energy bands in Al corresponding to the measured Fermi surface. [Energy is in units of  $(\hbar^2/2m^*) (2\pi/a)^2$ .] The bands along  $\Gamma L$  (not shown) are similar in form to the bands along  $\Gamma X$ . Expanded sections of this figure appear in Figs. 5 and 7.

in which the coefficients of the cubic form now explicitly depend on the reduced energy. The solutions to (10) are either

$$y = -(2/\sqrt{3})(4\epsilon + 2u^2 + \frac{1}{3})^{1/2} \times \cosh\left(\frac{1}{3} \operatorname{arccosh}\left[\frac{\sqrt{3}(4\epsilon + 5u^2 - \frac{1}{9})}{(4\epsilon + 2u^2 + \frac{1}{3})^{3/2}}\right]\right), \quad (11)$$

or

$$y = -(2/\sqrt{3})(4\epsilon + 2u^2 + \frac{1}{3})^{1/2} \times \cos\left[\frac{1}{3} \arccos\left(\frac{\sqrt{3}(4\epsilon + 5u^2 - \frac{1}{9})}{(4\epsilon + 2u^2 + \frac{1}{3})^{3/2}}\right)\right], \quad (12)$$

according to whether

$$\left|\frac{\sqrt{3}(4\epsilon + 5u^2 - \frac{1}{9})}{(4\epsilon + 2u^2 + \frac{1}{3})^{3/2}}\right| \geq 1.$$

In all but a small range of negative energies it is the 3 branches of (12) that are of interest and for these we have,

$$q_1(\epsilon) = [\epsilon + \frac{2}{3} - (2/\sqrt{3})(4\epsilon + 2u^2 + \frac{1}{3})^{1/2} \times (\frac{1}{2} \cos \frac{1}{3} \alpha(\epsilon) + (\sqrt{3}/2) \sin \frac{1}{3} \alpha(\epsilon))]^{1/2}, \quad (13a)$$

$$q_2(\epsilon) = [\epsilon + \frac{2}{3} - (2/\sqrt{3})(4\epsilon + 2u^2 + \frac{1}{3})^{1/2} \times (\frac{1}{2} \cos \frac{1}{3} \alpha(\epsilon) - (\sqrt{3}/2) \sin \frac{1}{3} \alpha(\epsilon))]^{1/2}, \quad (13b)$$

and

$$q_3(\epsilon) = [\epsilon + \frac{2}{3} + (2/\sqrt{3})(4\epsilon + 2u^2 + \frac{1}{3})^{1/2} \times \cos \frac{1}{3} \alpha(\epsilon)]^{1/2}, \quad (13c)$$

where

$$\alpha(\epsilon) = \arccos\left(\frac{\sqrt{3}(4\epsilon + 5u^2 - \frac{1}{9})}{(4\epsilon + 2u^2 + \frac{1}{3})^{3/2}}\right), \quad (14)$$

is defined in the range  $0 < \alpha < \pi$ . Geometrically,

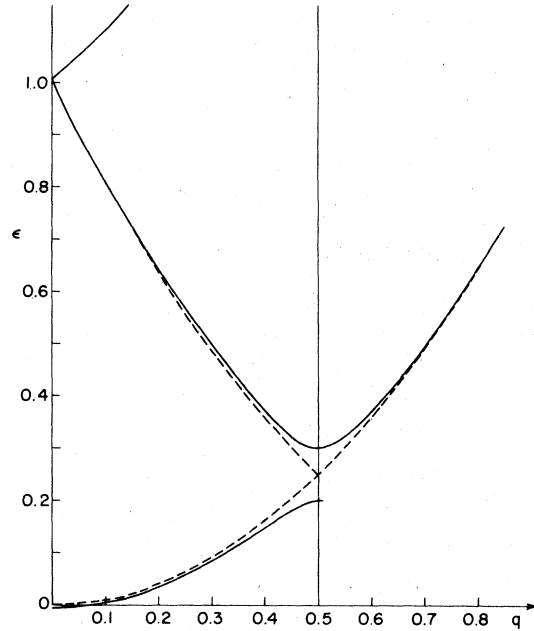


FIG. 3. Energy bands ( $k_{\perp}=0$ ) arising as solution to Eq. (9). The second band has been extended beyond  $q=\frac{1}{2}$  because as noted in the text a rotation of the figure by  $90^\circ$  gives the solution to the 3-band density of levels problem [relabeling  $q$  by  $g_m(e)$ ].

these solutions can be obtained from Fig. 3 by rotating it counterclockwise by  $90^\circ$  and reflecting about the (new) vertical axis. (One of the bands has been extended into the next zone for this purpose.)

If we now return to (5) [and use the definitions (6a) and (6c)] we find that

$$g_m(e) = (aK/2\pi)q_m(e/\gamma) \quad [\gamma = (aK/2\pi)^2]$$

and the deviations from free-electron behavior are thus

$$\Delta g_m(e) = (aK/2\pi)[q_m(e/\gamma) - (2\pi/aK)\sqrt{e}]. \quad (15)$$

It follows that in an approximation which neglects further structure arising from zone-plane interactions (see below) the density of levels can be obtained by augmenting  $\sqrt{e}$  with (15) summed over zone-plane pairs.<sup>11</sup>

An example of (15) augmented by the free-electron result is shown in Fig. 4 where the level density in aluminum is calculated in this approximation, the  $U_K$  being taken from Fermi-surface data.<sup>12</sup> Though quite different overall from Fig. 1(a) the principal features of the curve are very well understood: pairs of Van Hove cusps (square root singularities associated with band extrema) are separated by near linear regions in  $g(e)$ . The linear region, also expected from the general results of Van Hove,<sup>4</sup> can be traced to the follow-

ing: returning to equation (3) we note that the free-electron density of levels can be written

$$g(e) = [S(e)/S(1)]e^{-1/2}, \quad (16)$$

where  $S(e)$  is the area of a (spherical) constant energy surface at energy and  $S(1)$  is the area of a corresponding surface at  $e=1$  [i.e.,  $\epsilon = (\hbar^2/2m^*) \times (2\pi/a)^2$ ]. Suppose we now consider  $N_K$  pairs of equivalent Bragg planes (associated with reciprocal-lattice vector  $K$ ) which are cut by a spherical constant energy surface. The planes form a polyhedron inside of which there may be a portion  $S_K^i(e)$  of surface, and a portion  $S_K^o(e)$  outside. It is easy to show that

$$S_K^i(e)/S(1) = e(1 - N_K) + N_K(Ka/2\pi)e^{1/2}, \quad (17)$$

so that the contribution to the free-electron-level density from the portion of surface remaining inside the polyhedron is

$$g_K^i(e) = N_K(Ka/2\pi) - (N_K - 1)e^{1/2}.$$

Thus

$$g' = \left. \frac{dg_K^i(e)}{de} \right|_{e=\gamma} = -(N_K - 1) \frac{2\pi}{Ka}. \quad (18)$$

For the  $\{111\}$  planes of the fcc structure this slope is  $-\sqrt{3}$ , and for the  $\{200\}$  set it is  $-1$ . These are very close to the slopes seen in Fig. 4 between  $L_1$  and  $L_2'$ , and  $X_1$  and  $X_4'$ , respectively. The physical reason for this is that until the energy reaches  $L_2'$  (contact with the zone at  $L$  beginning at  $L_1$ ) no Fermi surface lies outside the  $\{111\}$  planes and that which is inside is predominantly free-electron-like.<sup>13</sup> A similar argument applies to the  $\{200\}$  planes except that it is necessary to note that when  $e$  reaches  $X_1$  the effects of the  $\{111\}$  set have largely healed. The argument readily generalizes to other structures.

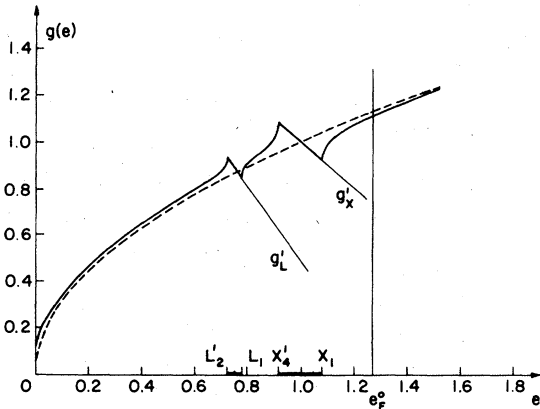


FIG. 4. Density of levels according to Eq. (15). The slopes  $g'_L$  and  $g'_X$  of the linear regions between the cusp structure are given in the text.

The form of the cusps bounding the linear region is well known from the two-band approximation.<sup>13</sup>

Define a vector  $\vec{l} = (l_x, l_y, l_z)$  by

$$\vec{l} = \vec{p} - \vec{K}(a/4\pi) \quad (\vec{l}_z \parallel \hat{K}).$$

Then

$$e = \frac{1}{4} + l^2 \pm [u^2 + (\vec{l} \cdot \hat{K})^2]^{1/2},$$

and for sufficiently small  $l_z$ ,

$$e \approx \frac{1}{4} + l_x^2 + l_y^2 \pm [u + (1/2|u|)l_z^2].$$

It follows that the singular part of the density of levels is [setting  $e_K = \frac{1}{4}(aK/2\pi)^2$ ]

$$\delta g(e) = \begin{cases} 2N_K |2u|^{1/2} (e_K - |u| - e)^{1/2}, & e < e_K - |u|, \\ 2N_K |2u|^{1/2} (e - e_K - |u|)^{1/2}, & e > e_K + |u|, \end{cases} \quad (19)$$

again in accordance with Van Hove's general results. Thus both the singular and linear forms of the density of levels resulting from zone contact of the constant energy surfaces can be straightforwardly accounted for and indeed are familiar results.

### III. ZONE-EDGE STRUCTURE

We shall now see that a very similar structure emerges when we consider the nature of the energy bands in the neighborhood of intersecting zone planes. As a rather specific example, which will illustrate some quite general points however, we shall examine the bands in the vicinity of the intersection of two  $\{111\}$  planes in the fcc zone [see Fig. 1(b)]. Near the point  $K$  [i.e.,  $\vec{k}_K = (2\pi/a)(\frac{3}{4}, \frac{3}{4}, 0)$ ] and near the points equivalent to  $K$  by symmetry the bands follow from the solutions of<sup>14</sup>

$$\begin{vmatrix} T_0(\vec{k}) & U_1 & U_1 \\ U_1 & T_{111}(\vec{k}) & U_2 \\ U_1 & U_2 & T_{11\bar{1}}(\vec{k}) \end{vmatrix} = 0, \quad (20)$$

where  $U_1 = U(111)$ ,  $U_2 = U(200)$ , and  $U_1 \neq U_2$ . Again we anticipate second-order corrections to these solutions from higher bands. We may reduce (20) as follows: put

$$\vec{k} = \vec{k}_K + (2\pi/a)\vec{\kappa}.$$

Then (20) can be written

$$\begin{vmatrix} 2\sqrt{2}q - \lambda & u_1 & u_1 \\ u_1 & -2p - \lambda & u_2 \\ u_1 & u_2 & 2p - \lambda \end{vmatrix} = 0, \quad (21)$$

where

$$q = \vec{\kappa} \cdot (1/\sqrt{2}, 1/\sqrt{2}, 0), \quad (22a)$$

$$p = \vec{\kappa} \cdot (0, 0, 1), \quad (22b)$$

and

$$\lambda = e - \frac{9}{8} - \kappa^2 + (1/\sqrt{2}) \vec{\kappa} \cdot (1/\sqrt{2}, 1/\sqrt{2}, 0). \quad (22c)$$

(As before energies are measured in units of  $\epsilon_X^0$ .)  
Expanding (21) we now arrive at

$$(2\sqrt{2}q - \lambda)(\lambda^2 - u_2^2 - 4p^2) + 2u_1^2(u_2 + \lambda) = 0. \quad (23)$$

An equation similar to this will result for a structure other than fcc providing variables exploiting the symmetry and corresponding to (22a) and (22b) are used.

Let us first consider solutions to (23) for the case  $p=0$ , i.e.,  $\vec{\kappa}$  confined to the (mirror) plane (100). From the three nondegenerate values of  $\lambda$  so obtained, we find

$$e_1 = \frac{9}{8} + \kappa^2 - (1/\sqrt{2})q - u^2, \quad (24)$$

$$e_2 = \frac{9}{8} + \kappa^2 + (1/\sqrt{2})q + \frac{1}{2}u_2 + [(\sqrt{2}q - u_2/2)^2 + 2u_1^2]^{1/2}, \quad (25)$$

and

$$e_3 = \frac{9}{8} + \kappa^2 + (1/\sqrt{2})q + \frac{1}{2}u_2 - [(\sqrt{2}q - u_2/2)^2 + 2u_1^2]^{1/2}. \quad (26)$$

These bands are plotted in Fig. 5. The important point to notice in these curves is that  $e_2$  gives rise to a band minimum and  $e_3$  to a band maximum, but these extrema are not located at the  $K$  point ( $\vec{\kappa}=0$ ), nor are they coincident in the zone (as, for example, are the extrema considered earlier). The  $K$  point can be considered to lie on the line of symmetry  $\Gamma K$  extended by  $K\bar{X}$  to  $\bar{X}$ , a center of a square face in a bordering zone. Though this line lies in a plane of reflection symmetry, there is no inversion symmetry (about  $K$ ) along it. Band

extrema may therefore be located on the line of symmetry but not necessarily at  $K$  itself. In fact it is easy to see that the minimum in  $e_2$  [ $e_2(\min)$ ] is at

$$q = q_{\min} = (1/2\sqrt{2})u_2 - (1/\sqrt{3})|u_1|; \quad (27)$$

whereas the maximum in  $e_3$  [ $e_3(\max)$ ] is at

$$q = q_{\max} = (1/2\sqrt{2})u_2 + (1/\sqrt{3})|u_1|. \quad (28)$$

The extrema are therefore separated in energy by

$$\Delta e = e_2(\min) - e_3(\max) = \sqrt{6}|u_1|, \quad (29)$$

plus second-order corrections.

Since (23) is quadratic in  $p$  we immediately anticipate singular structure in the density of levels associated with these extrema. It will be in the form of a Van Hove pair, with cusps separated by  $\sqrt{6}|u_1|$  (which may be contrasted with the separations  $2|u_1|$  or  $2|u_2|$  for the zone-plane structure). Again, to within second-order corrections the cusps are equidistant from a mean energy

$$\bar{e} = \frac{9}{8} + \frac{3}{4}u_2. \quad (30)$$

To complete the description of these singularities we need to determine the curvature of  $e_i$  at the extrema. This is easily accomplished by expanding (23). The result is that on the high- and low-energy sides of

$$\frac{9}{8} + \frac{3}{4}u_2 \pm (3/\sqrt{2})|u_1|, \quad (31)$$

[referred to as  $A_u(+)$  and  $A_l(-)$ ] we expect a square-root behavior in  $g$ . In the fcc structure the basic integration over  $k$  required for  $G(\delta)$  can be restricted to the  $\frac{1}{16}$ th symmetry element of the zone which contains at two of its corners the (equiva-

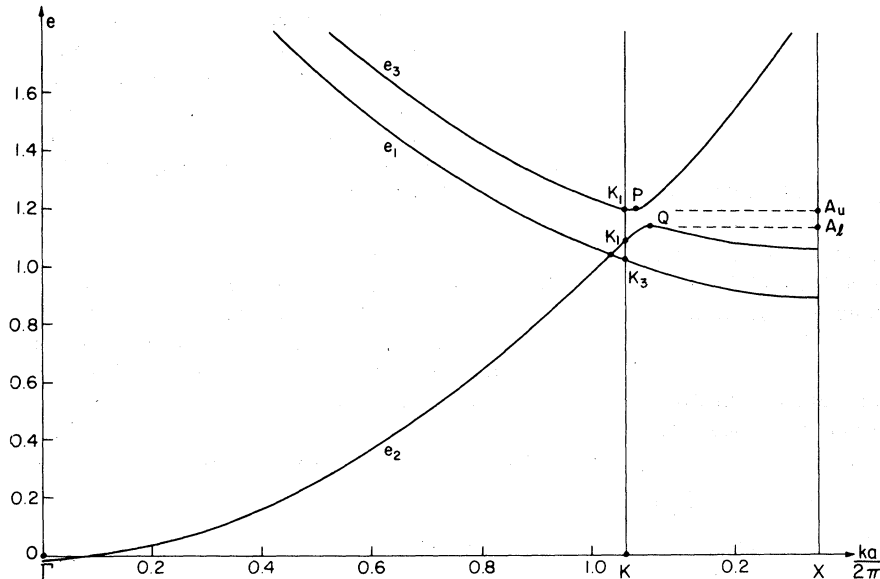


FIG. 5. Energy bands along  $\Gamma K$  and  $KX$ : Note that the positions of the extrema (marked  $P$  and  $Q$  at energies  $A_l$  and  $A_u$ ) do not coincide with the symmetry point levels  $K_i$ . Also note the band contact near the  $K$  point. Bands  $e_1$ ,  $e_2$ , and  $e_3$  are given by Eqs. (24), (25), and (26), respectively.

lent) points  $U$  and  $K$ , each of which is shared by three neighboring zones. Accounting for the mirror planes we therefore arrive at a weight of 16 for each such singularity: this plays the role of the  $N_K$  for the zone-face structure considered above. Then if  $\Delta e$  is measured from the energies given in (31) we find

$$\delta g(\Delta e) = 8 \left( \frac{2\sqrt{2}}{3^{7/8}} \right) (|u_1||u_2 + |u_1|/\sqrt{6}|)^{1/2} \sqrt{\Delta e}, \quad (32)$$

for an energy  $\Delta e$  in excess of the band minimum, and

$$\delta g(\Delta e) = 8 \left( \frac{2\sqrt{2}}{3^{7/8}} \right) (|u_1||u_2 - |u_1|/\sqrt{6}|)^{1/2} \sqrt{\Delta e}, \quad (33)$$

for an energy  $\Delta e$  below the band maximum. If  $|u_1| \ll u_2$  (as in Al) it is possible to replace these by

$$\delta g(\Delta e) = 8 \left( \frac{2\sqrt{2}}{3^{7/8}} \right) (|u_1 u_2|^{1/2}) \sqrt{\Delta e}. \quad (34)$$

It remains to determine the linear region in  $g(e)$  between these two cusps. By an argument similar to the one used to determine  $g(e)$  between  $L_1$  and  $L'_2$  (or  $X_1$  and  $X'_4$ ), we note that when  $e$  falls in the gap near  $K$  [see Eq. (29)] the structure of  $g(e)$  is determined largely by the free-electron contribution elsewhere. For energies confined to this gap it is the case that first and second zone levels are occupied, while third zone levels are empty. The third zone area is missing and the total area is that of the first and second zones. For a free-electron surface it is a matter of simple geometry to calculate the third zone area when  $e$  is in excess of  $\frac{9}{8}$  by a small amount, i.e.,

$$e = \frac{9}{8} + \delta,$$

where  $\delta$  is small. The result certainly must be of the form

$$S_3 = C_{fcc} \delta^{3/2},$$

since the third zone sections of the free-electron Fermi surface can be constructed, approximately, from three planar sections each composed of two triangular regions whose heights scale as  $\delta^{1/2}$  and whose bases as  $\delta$ . The constant  $C_{fcc}$  is determined from a simple argument: observe that when  $\delta \leq \frac{1}{8}$  the total Fermi surface area is divided among zones 1, 2, and 3 there being none in zone 4, i.e.,

$$S = S_1 + S_2 + S_3.$$

When  $e = \frac{5}{4}$  (i.e.,  $\delta = \frac{1}{8}$ ) the Fermi surface exactly passes through the  $W$  point and then both zone 1 and zone 4 are empty. Thus

$$S(e = \frac{5}{4}) = S_2 + S_3 = 4\pi k^2. \quad (35)$$

But from a slight extension of (17) it is easy to see that

$$S_2 + 2S_3 = 4\pi k^2 [N_{K_1}(1 - K_1/2k) + N_{K_2}(1 - K_2/2k)], \quad (36)$$

where  $N_{K_1}$  and  $N_{K_2}$  are the numbers of zone-plane pairs corresponding to reciprocal-lattice vectors  $K_1$  ( $\{111\}$ ) and  $K_2$  ( $\{200\}$ ). From (35) and (36) we deduce that when  $\delta = \frac{1}{8}$  ( $k = \sqrt{5}/2$ ) we have

$$S_3 = 4\pi k^2 [4(1 - \sqrt{3}/2K) + 3(1 - 1/k) - 1],$$

or

$$S_3/S = 6(1 - 1/\sqrt{5} - 2/\sqrt{15}) = 0.2183, \quad (37)$$

an exact determination of the third zone area for  $e = \frac{5}{4}$ . It then follows that

$$S_3(k = \sqrt{5}/2) = 3.429 = C_{fcc}(\delta)^{3/2} \quad (\delta = \frac{1}{8}),$$

or

$$S_3 = 77.6 \delta^{3/2}, \quad (38)$$

the constant  $C_{fcc} = 77.60 = 480\sqrt{2}\pi(1 - 1/\sqrt{5} - 2/\sqrt{15})$ , being uniquely related to the zone geometry.<sup>15</sup>

This result, combined with Eq. (16), enables us to obtain an estimate for the slope of  $g(e)$  either side of the cusps described by (34). For, if  $e$  is within the gap near  $K$ , then

$$g(e) \approx \frac{4\pi e - C_{fcc}\delta^{3/2}}{4\pi e^{1/2}}, \quad (39)$$

so that for small values of  $\delta$

$$\frac{dg(e)}{de} \approx \frac{1}{2e^{1/2}} - \frac{3}{2} \frac{C_{fcc}}{4\pi} \frac{\delta^{1/2}}{e^{1/2}}. \quad (40)$$

In the case of Al this leads to slopes of approximately  $-1.1$  at the lower cusp,  $-2.1$  at the upper, and  $-1.7$  at the gap center. This variation across the gap reflects the nonanalytic growth of the free-electron third zone area, an effect not encountered at lower energies in the first and second zones. Rounding of the actual Fermi surface, not accounted for in (39) will ameliorate some of this variation in slope, and since such rounding is less important the higher is  $\delta$ , we can expect the value of  $dg/de$  at the upper extent of the gap to be the more reliable estimate, i.e.,

$$g' \approx (\sqrt{2}/3)[1 - (3C_{fcc}/8\pi)][u_2 + (1/\sqrt{6})|u_1|]^{1/2}. \quad (41)$$

Referring to Fig. 6(a) we may therefore summarize to this point as follows: the principal singular structure in  $\delta g(e)$  can be located by the energies  $L'_2$  and  $L_1$  ( $\mathcal{E}_L^\pm |V_{111}|$  to first order),  $X'_4$  and  $X_1$  ( $\mathcal{E}_X^\pm |V_{200}|$  to first order) and  $A_1$  and  $A_4$  [ $\mathcal{E}_K^\pm + \frac{3}{4}V_{200} \pm (3/\sqrt{2})|V_{110}|$  to first order]. The magnitude of the singular structures, given these energies, is determined very nearly by the slopes  $g'_L$ ,  $g'_X$ , and  $g'_K$  [Eq. (18) and (41)]. Immediately below or above each singular point we find that  $\delta g \sim (\Delta e)^{1/2}$  with coefficients given according to

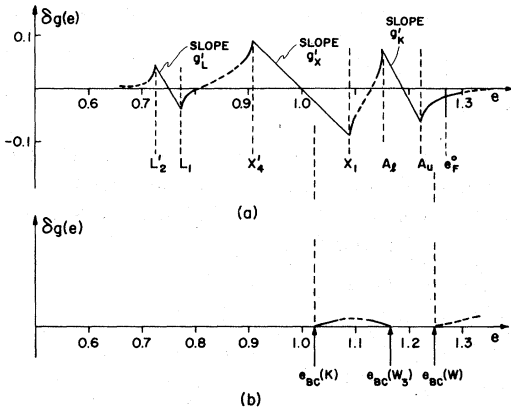


FIG. 6(a) Summary of cusp structure in the normalized density of levels arising from singular points in the band structure near  $L$ ,  $X$ , and  $K$ . Notice that the energy gaps and slopes ( $g'$ ; see text) determine the magnitudes  $\delta g$ . Notice also the significant departure from free-electron behavior at  $e_F$ . (b) Structure in  $\delta g$  associated with the singular critical points (see text) near  $W$  and  $K$ . Here  $e_{BC}(K)$  and  $e_{BC}(W_3)$  mark the location of minimum and maximum energies on the closed loop along which bands one and two touch. Bands two and three begin to touch at  $e_{BC}(W)$ , also a minimum. The closed loop (see text) along which these bands meet will also have a maximum, in this case at an energy much greater than  $e_F$ .

case by Eqs. (32) and (40). [Notice from Fig. 6(a) that between  $L_1$  and  $A_u$ , there is then very little freedom in constructing continuous curves between the singularities.] The other point worth noticing immediately here is that residual structure from  $A_u$  persists quite noticeably at the free-electron Fermi energy.<sup>16</sup> This point gains further prominence when we consider the additional single-particle structure in  $g(e)$  that arises from band contact.

#### IV. BAND-CONTACT STRUCTURE

We have not, however, exhausted the possible singular structures. There are three other minor features occurring, as indicated earlier, in the energy range of interest here ( $\mathcal{E} \lesssim \mathcal{E}_F^0$ ). They are associated with the occurrence of contact between bands, which can be seen happening near the  $W$  point and also at the  $K$  point (Figs. 5 and 7). These are examples of the behavior expected from the general arguments of Herring<sup>17</sup> concerning accidental degeneracy. To elucidate the nature of the energy bands in the neighborhood of such degeneracies we consider first a wave vector  $\vec{k}$  in the vicinity of  $W$  [ $\vec{k}_W = (2\pi/a)(1, \frac{1}{2}, 0)$ ] where the secular equation can be written<sup>7</sup>

$$(t_0 t_{200} - u_2^2)(t_{111} t_{11\bar{1}} - u_2^2) - u_1^2(t_0 + t_{200} - 2u_2)(t_{111} + t_{11\bar{1}} - 2u_2) = 0, \quad (42)$$

with

$$T_i = t_i \mathcal{E}_X^0.$$

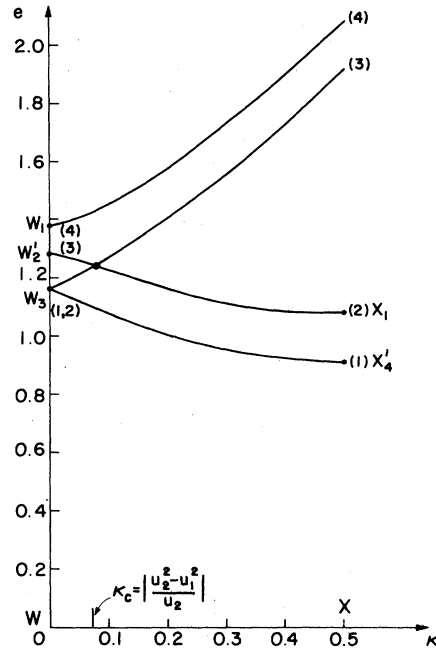


FIG. 7. Energy bands along  $WX$ . First and second bands are degenerate at  $W$ , split as  $K$  moves towards  $X$ , and the upper member of the pair crosses a band which at  $W$  is counted as third, but at  $X$  is second. Numbers in parentheses give band indices (Ref. 19).

If we put

$$\vec{k} = \vec{k}_W + \vec{\kappa}'(2\pi/a),$$

then we find

$$t_{111} = t_0 - 2\vec{\kappa}' \cdot (1, 1, 1),$$

$$t_{11\bar{1}} = t_0 - 2\vec{\kappa}' \cdot (1, 1, \bar{1}),$$

and

$$t_{200} = t_0 - 2\vec{\kappa}' \cdot (2, 0, 0).$$

Now as Harrison<sup>18</sup> has noted, curves of band contact in Al will lie, by symmetry, in (100) planes; these are planes of reflection. In such a plane  $\kappa'_z = 0$ , and it follows that along a curve confined in the plane

$$t_{111} = t_{11\bar{1}}.$$

Then from (42) either

$$t_{111} = u_2 \quad (43)$$

or

$$(t_0 t_{200} - u_2^2)(t_{111} + u_2) - 2u_1^2(t_0 + t_{200} - 2u_2) = 0. \quad (44)$$

But in order for the band given by (43) to be simultaneously degenerate with one of the bands given by (44) we must have

$$\kappa_y'^2 + \kappa_y' [(u_2^2 - u_1^2)/u_2] = \kappa_x'^2, \quad (45)$$

a result also obtained by Harrison.<sup>18</sup> It follows that Eq. (45) (augmented with the condition  $\kappa_z' = 0$ )

gives the curves (and symmetry determined replicas) along which bands touch. In a more complete treatment involving an infinite-order secular equation we can expect the curves represented by (45) to be but portions of closed curves (approximating the shape of a rounded square) along which the energy may have extrema.

The hyperbola represented by (45) has two branches, one of which passes through the point  $W$  where, as is well known, there is a double degeneracy (see Fig. 7). For the choice of  $u_1$  and  $u_2$  used in our example, the degeneracy involves bands one and two. We may easily trace this branch of the hyperbola to the  $K$  point (see Fig. 5) as follows: near  $K$  (and for  $k_z=0$ ) we may write  $\vec{k} = (2\pi/a)[\vec{k} + (\frac{3}{4}, \frac{3}{4}, 0)]$  and use (20) to find the line of band contact. Its equation is

$$\kappa_y = -\kappa_x - (u_2^2 - u_1^2)/2u_2,$$

and accounting for the change in origin (from  $W$  to  $K$ ) this is simply the asymptote of the branch of (45) that passes through  $W$ . Accordingly bands 1 and 2 touch along this branch: bands 2 and 3 touch along the other branch, as can be seen from Fig. 7.

For the purposes of locating (in energy) the singular structure in  $g(e)$  associated with band contact, we need to determine the energy at which bands *first* touch. Using the solution  $t_{111} = u_2$  it follows that

$$e = k_K^2 - \frac{1}{2}(\kappa_x + \kappa_y) + (\kappa_x^2 + \kappa_y^2) - u_2,$$

so that along the line of band contact the minimum value is

$$e_{BC}(K) = k_K^2 - u_2 + (u_2^2 - u_1^2)/4u_2 + \frac{1}{2}[(u_2^2 - u_1^2)/2u_2]^2. \quad (46)$$

This indicates the onset of band contact near  $K$ , and is marked as such on Fig. 6(b). The corresponding band-contact *maximum* on this branch is at  $W$ . We refer to it as  $e_{BC}(W_3)$  [Fig. 6(b)]. There is also a band-contact minimum near  $W$  associated with the remaining branch of (45). It is easily seen to be located at

$$\vec{k}'_c = (0, \kappa_c, 0),$$

where

$$\kappa_c = -(u_2^2 - u_1^2)/u_2$$

(measured from  $W$ ). From (43) the corresponding energy is found to be

$$e_{BC}(W) = e_w + [(u_2^2 - u_1^2)/u_2]^2 - u_1^2/u_2, \quad (47)$$

and is also marked in Fig. 6(b).

It remains to investigate the nature of the singular structure in  $g(e)$  associated with  $e_{BC}(K)$  and  $e_{BC}(W)$ .

We consider the latter; the arguments for  $e_{BC}(K)$  and  $e_{BC}(W_3)$  are almost identical. We proceed from (42), first writing

$$\vec{k}' = \vec{k} + \vec{k}'_c, \quad (48)$$

where  $\vec{k}'$  was previously measured from  $W$ . The wave vector  $\vec{k}$  is now measured from the location of initial-band contact and is taken to be small. After a little algebra we find

$$\begin{aligned} t_0 &= \Delta + \kappa_y + 2\kappa_c + 2\kappa_x, \\ t_{200} &= \Delta + \kappa_y + 2\kappa_c - 2\kappa_x, \\ t_{111} &= \Delta - \kappa_y - 2\kappa_x, \\ t_{11\bar{1}} &= \Delta - \kappa_y + 2\kappa_x, \end{aligned} \quad (49)$$

where

$$\Delta = e_{BC}(W) - e + u_2 + \kappa^2 + 2\kappa_y\kappa_c. \quad (50)$$

Using transformation (48) the curves of band contact are given by

$$\kappa_y^2 + \kappa_y\kappa_c = \kappa_x^2 \quad (\kappa_z = 0), \quad (51)$$

and if  $\kappa_x$  is small enough we can write

$$\kappa_y \approx \kappa_x^2/\kappa_c. \quad (52)$$

Evidently there is no discontinuity in  $\nabla_{\kappa_x} e$  at the band-crossing minimum.

Now if  $\vec{k}$  is confined to the line  $XW$  (which implies  $t_0 = t_{200}$ , and  $t_{111} = t_{11\bar{1}}$ ) then (42) reduces to

$$(t_0 + u_2)[t_0 + u_2 - 2(\kappa_y - \kappa_c)] = 4u_1^2,$$

or

$$\Delta + \kappa_y + 2\kappa_c = (\kappa_y - \kappa_c) + [(\kappa_y - \kappa_c)^2 + 4u_1^2]^{1/2}$$

and

$$\Delta + \kappa_y + 2\kappa_c = (\kappa_y - \kappa_c) - [(\kappa_y - \kappa_c)^2 + 4u_1^2 - u_2]^{1/2}. \quad (53)$$

It is this last band that crosses the band corresponding to  $t_0 = u_2$ , the degeneracy occurring at  $\kappa_y = 0$  (see also, Fig. 7). If standard band ordering is now imposed<sup>19</sup> it follows that a discontinuity in  $\nabla_{\kappa_y} e$  occurs at  $\kappa_y = 0$ .

Next, consider wave vectors  $\vec{k}$  confined to the (200) face passing through the point  $W$  under consideration. Then  $\kappa_x = 0$ ,  $\kappa_y, \kappa_z \neq 0$ , and one solution of (42) is  $t_0 = u_2$ . For the energy range of interest, the others are given by

$$\delta^2 + \frac{2\delta u_2(u_2\kappa_y - \kappa_z^2)}{u_1^2 + u_2^2} - 4\kappa_z^2 \frac{u_1^2 + u_2\kappa_y}{u_1^2 + u_2^2} = 0, \quad (54)$$

where

$$\delta = \Delta - \kappa_y - u_2.$$

This is sufficient to establish that when  $\kappa_y = 0$  there are two solutions for  $\delta$  (and hence for  $e$ ) that are

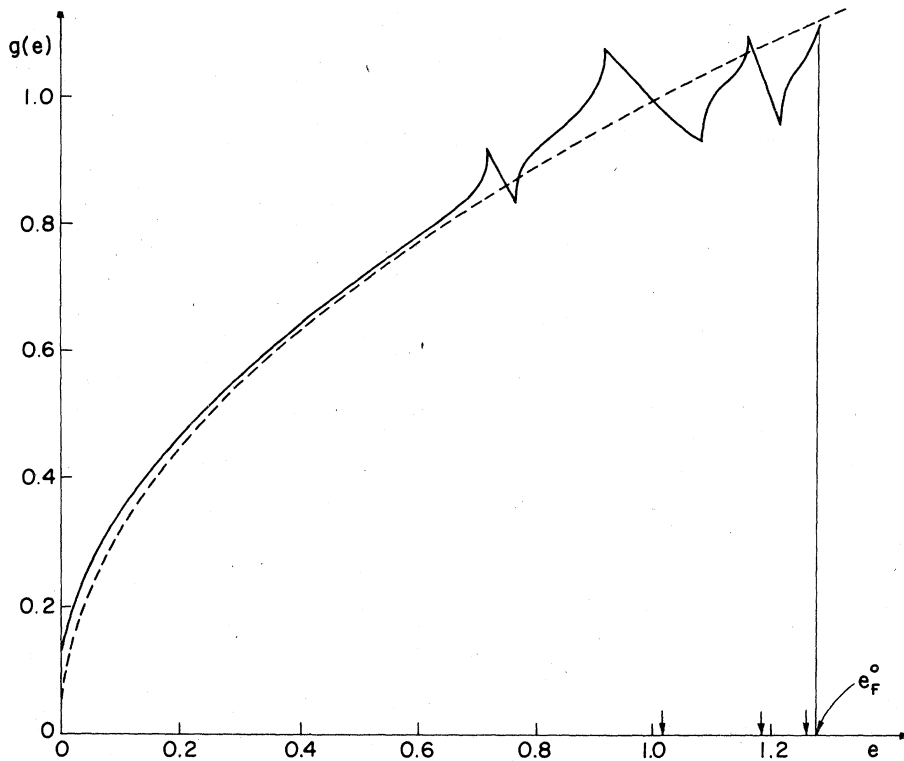


FIG. 8. One-electron density of levels in Al for  $e < e_F^0$ . The curve shows the major cusp structure and minor features (arrows) reflecting critical points on band-contact curves. Each of these contributes  $\delta g \sim (\delta e)^{3/2}$  (see text) and the one closest to  $e_F$  is partially responsible for the steeply rising behavior of the density of levels at the Fermi energy.

linear in  $\kappa_z$ . Accordingly at  $e_{BC}(W)$ ,  $\nabla_{\kappa_z} e$  is also discontinuous. We may now conclude that the  $k$ -space point corresponding to  $e_{BC}(W)$  is one at which there are two discontinuous components of  $\nabla_{\mathbf{k}} e$ , but is also a point lying on a curve of contact between two bands. It is an example of a singular critical point, as discussed by Phillips,<sup>5</sup> for which

$$\delta g \sim (e - e_{BC})^{3/2}. \quad (55)$$

This behavior is indicated schematically in Fig. 6(b). Because of the relatively small phase space involved with these singular points we may expect their overall contribution to  $\delta g$  to be somewhat smaller than that expected from the cusp structures, but to determine their overall magnitude it may be necessary to defer to numerical computation. Figure 8 (which shows the density of levels with all important singular features represented) includes a crude estimate of the contributions from  $e_{BC}(K)$  and  $e_{BC}(W)$  by considering the  $k$ -space volumes involved in the small conical parts of the corresponding constant energy surfaces surrounding the points. Note however that the location in energy of the band-contact critical points is readily determined.

This completes the analysis of those singular contributions to  $g(e)$  at energies less than  $e_F$ . Arguments of a similar kind can be advanced to reveal the nature of singular structure at energies

in excess of  $e_F$  (e.g., at  $W_2'$  and  $W_1$ ) and also, as noted earlier, for different crystal structures.

## V. DISCUSSION

We have shown by example that for a nearly-free-electron metal whose energy bands can be described by a pseudopotential interpolation, the principal structure of the one-electron density of levels can be located in terms of the major pseudopotential components. Though it is possible to estimate the contribution of the dominant singular regions, it would be useful to have confirmation of the estimates by numerical means<sup>20</sup> that nowadays are of an accuracy sufficient to determine even the weak features associated with the band contacts.<sup>21</sup> Such a feature can be seen near the Fermi energy in the calculation of Smrčka<sup>22</sup> but is not identified as such. The same calculation clearly shows a zone-edge cusp pair near the  $K$  point (though there seem to be no extrema along  $KX$  in the published bands): Smrčka attributes this structure to band crossing, which appears to be a misinterpretation. Both zone-edge and band-contact features are clearly apparent in the density of levels calculation of Koyama and Smith<sup>23</sup> a determination based on the band structure compatible with the known Fermi surface<sup>7</sup> of Al. Other calculations<sup>24-30</sup> of the valence-level density for Al

in the energy range of interest here show similar structure to varying degrees depending largely on the accuracy of the method used.

Zone-edge structure in  $g(e)$  might well be apparent in certain experimental probes, notably soft-x-ray emission. The  $L_{23}$  emission data of Neddermeyer<sup>31</sup> shows features that may be readily identified with  $A_u$  and  $A_l$  and is more clearly resolved than the  $L_1$ ,  $L'_2$  structure. The same is true of the data of Fuggle *et al.*,<sup>32</sup> and the point may be made that the zone-edge pair of singularities can be used to determine  $V_{111}$  with far more precision [see Eq. (29)] than the lower energy structure. The other point worth making is that the density of levels at  $e_F$ , while close in magnitude to free-electron value, is nevertheless highly peaked there, and this is entirely due to single-particle effects, namely, those associated with  $A_u$  and  $e_{BC}(W)$ . Figure 8 makes this apparent by showing the termination of  $g(e)$  by a zero temperature Fermi-Dirac function. In an experiment, thermal broadening and instrumental resolution will pare the high-energy side of this peak further. Evidently the extraction of information pertaining to x-ray absorption or emission-edge many-body structure<sup>33</sup> will require that the single-particle structure near  $e_F$  be properly determined, especially that arising from a neighboring band contact  $\delta g \sim (\Delta e)^{3/2}$  region.

As remarked earlier, the square root singularities associated with zone-edge structure are separated as far as their  $k$ -space locations are concerned. In the case of fcc Al, we see from (27) and (28) that the two corresponding extreme be along the  $XW$  line of the zone (a [100] direction) and are separated by

$$\Delta q = (2/\sqrt{3})|u_1|. \quad (56)$$

It will be recalled that the energy separation of the critical points is  $\sqrt{6}|u_1|$ . Restoring the appropriate dimensional factors, the change in wave vector corresponding to (56) is

$$\frac{2\pi}{a} \frac{2}{\sqrt{3}} \frac{V_{111}}{g_x^0},$$

or about  $0.05 \text{ \AA}^{-1}$  in Al. Evidently the points  $A_u$  and  $A_l$  may jointly be scanned by a probe (electron energy loss, for example) capable of resolving an excitation of 0.58 eV at a momentum transfer of  $0.05 \text{ \AA}^{-1}$ .

It is of interest to enquire whether the upper cusp of the zone-edge structure (at  $A_u$ ) may be brought by an application of pressure to the Fermi energy, and thereby possibly make its influence felt more prominently in both equilibrium and transport properties, or even perhaps in ordered states such as superconductivity. A first-order analysis

shows that for this to happen we must have

$$e_F = \frac{9}{8} + \frac{3}{4}u_2 + (3/\sqrt{2})|u_1|, \quad (57)$$

where in computational units  $e_F = 1.269$  (plus second-order corrections). If we determine the  $u$ 's from a screened empty-core pseudopotential whose core radius  $r_c$  is taken as an invariant property of the aluminum ion,<sup>34</sup> then setting  $x = q/2k_F$  we have

$$u(x) = -\frac{2}{3} \left( \frac{\epsilon_F}{\epsilon_x} \right) \frac{\lambda^2 \cos sx}{x^2 + \lambda^2 f(x)},$$

where  $s = 2k_F r_c$ ,  $\lambda^2 = 0.166 r_c$  (recall that  $k_F a_0 r_s = 1.92$ ), and  $f(x)$  is an exchange and correlation correction to the dielectric function of the electron gas, whose exact form is not at all important for the present estimate. An increase in pressure decreases the value of electron spacing parameter  $r_s$  and hence alters the values of  $u(x_{111})$  and  $u(x_{200})$ . Since the argument of the cosine is close to  $\pi/2$  we can deduce that

$$du(x)/dr_s \approx [u(x)/r_s^0](1 + s_0 x \tan s_0 x),$$

where  $r_s^0$  is the appropriate zero-pressure value. Thus

$$u(x, r_s)$$

$$\approx u(x, r_s^0) + [u(x, r_s^0)/r_s^0](1 + s_0 x \tan s_0 x) \Delta r_s.$$

Condition (57) then determines  $|\Delta r_s|/r_{s0}$  to be approximately 0.035 (thus  $\Delta V/V \sim 0.1$ ) which translates with the known bulk modules of Al to a pressure less than 100 kbar. This assumes that Al remains in the fcc structure, which according to the calculations of Friedli and Ashcroft<sup>35</sup> is likely to be the case. If the singular point is manifested in a physical property of the metal at an accurately determined pressure, such a measurement will aid not only in the verification of the band structure, but also will serve to determine the volume dependence of the pseudopotential. This principle should apply in other polyvalent metals, and also in intermetallics with sufficiently high nominal valence.

## VI. ACKNOWLEDGMENTS

This work has received support from the NSF through Grant No. DMR-77-18329 which is gratefully acknowledged.

## APPENDIX

The branches of the arccosine in (9) are easily ordered by considering the solutions at a zone plane ( $q = \frac{1}{2}$ ). Then

$$y = (2/\sqrt{3})4/\sqrt{3} + 2u^2 \cos \left\{ \frac{1}{3} \arccos \left[ \frac{\sqrt{3}(\frac{8}{9} - u^2)}{(\frac{4}{3} + 2u^2)^{3/2}} \right] \right\}, \quad (\text{A1})$$

and when  $u \rightarrow 0$  the solutions corresponding to  $\cos^{-1}(-1) = \pi, -\pi$ , and  $3\pi$ , and  $\epsilon = \frac{1}{4}, \frac{1}{4}$ , and  $\frac{9}{4}$ , as required. If  $u \neq 0$ , the solutions may be written

$$y_m = (2/\sqrt{3})4/\sqrt{3} + 2u^2 \cos \left[ \frac{1}{3} \pi - \frac{1}{3} \alpha \left( \frac{1}{2} \right), \pm \frac{1}{3} 2\pi \right] \quad (m = 1, 2, 3), \quad (\text{A2})$$

where

$$\sin \alpha \left( \frac{1}{2} \right) = \frac{|4u| \left( 1 + \frac{13}{18} u^2 + \frac{1}{2} u^4 \right)^{1/2}}{\left( \frac{4}{3} + 2u^2 \right)^{3/2}}. \quad (\text{A3})$$

The first-order energies are therefore

$$\epsilon_1 = \frac{1}{4} - |u|, \quad \epsilon_2 = \frac{1}{4} + |u|, \quad \epsilon_3 = \frac{9}{4}, \quad (\text{A4})$$

again, as required. Corrections to (A4) higher order in  $|u|$  can be readily obtained by further expansion of (A3). Away from the zone plane ( $q < \frac{1}{2}$ ) the energies are

$$\begin{aligned} \epsilon_1 &= q^2 + \frac{2}{3} - (2/\sqrt{3})(4q^2 + 2u^2 + \frac{1}{3})^{1/2} \\ &\quad \times \left[ \frac{1}{2} \cos \frac{1}{3} \alpha(q) + \frac{1}{2} \sqrt{3} \sin \frac{1}{3} \alpha(q) \right], \\ \epsilon_2 &= q^2 + \frac{2}{3} - (2/\sqrt{3})(4q^2 + 2u^2 + \frac{1}{3})^{1/2} \\ &\quad \times \left[ \frac{1}{2} \cos \frac{1}{3} \alpha(q) - \frac{1}{2} \sqrt{3} \sin \frac{1}{3} \alpha(q) \right], \\ \epsilon_3 &= q^2 + \frac{2}{3} + (2/\sqrt{3})(4q^2 + 2u^2 + \frac{1}{3}) \cos \frac{1}{3} \alpha(q), \end{aligned}$$

where

$$\cos \alpha(q) = \frac{\sqrt{3} x}{(x+a)^{3/2}}, \quad x = 4q^2 - u^2 - \frac{1}{9},$$

and

$$a = 2u^2 + \frac{4}{9}.$$

Away from a zone plane, a wave vector can always be specified in part by a polar angle measured from  $\hat{K}$ . It follows therefore that for fixed values of this angle and for fixed energy, the magnitude the wave vector can be determined in this symmetric three-plane wave model. By this means, Fermi-surface dimensions can be obtained.

<sup>1</sup>For a review of these methods, see M. L. Cohen and V. Heine, *Solid State Phys.* 24, 38 (1970).

<sup>2</sup>W. A. Harrison, *Phys. Rev.* 147, 467 (1966); A. I. Golovashkin, A. I. Kopelovich, and G. P. Motulevich, *Sov. Phys. JETP* 26, 1161 (1968); N. W. Ashcroft and K. Sturm, *Phys. Rev. B* 3, 1898 (1971).

<sup>3</sup>K. Sturm and N. W. Ashcroft, *Phys. Rev. B* 10, 1343 (1974).

<sup>4</sup>L. Van Hove, *Phys. Rev.* 89, 1189 (1953).

<sup>5</sup>J. C. Phillips, *Phys. Rev.* 104, 1263 (1956).

<sup>6</sup>Real simple metals are never strictly periodic: even if both pure and without defects they suffer distortions from the presence of phonons which means, for example, that the actual Fourier components of pseudopotentials extracted from experimental measurement may contain Debye-Waller type correction factors.

<sup>7</sup>N. W. Ashcroft, *Philos. Mag.* 8, 2055 (1963). The band structure taken from this reference corresponds closely to the measured Fermi surface. (Note, however, that two of the bands along  $\Gamma U$  have been reversed in connecting the discrete solutions of the secular equation used there. This is corrected in Fig. 2.) Slightly refined parameterization was proposed by Anderson and Lane [*Phys. Rev. B* 2, 298 (1970)] which may yet be further refined by more recent high-precision measurements of the Fermi surface of Al [Coleridge and Holtham, *J. Phys. F* 7, 1891 (1977)].

<sup>8</sup>It is assumed that  $|U_{2\mathbf{K}}| < |U_{\mathbf{K}}|$ , as is usually the case. Effects of  $U_{2\mathbf{K}}$  begin at second order and can be accounted for by a further application of perturbation theory.

<sup>9</sup>See, for example, *Solid State Physics* by N. W. Ashcroft and N. D. Mermin (Holt, New York, 1976) p. 156.

<sup>10</sup>See Ref. 9, p. 143.

<sup>11</sup>To second order in  $U_{\mathbf{K}}$  it is sufficient to assume the effects of zone planes, taken in symmetric pairs, to be

additive. This is a consequence of perturbation theory and also of (3) written in its equivalent form  $G_m(\mathcal{E}) = \sum_{\mathbf{k} \in \text{BZ}} \delta(\mathcal{E} - \mathcal{E}_m(\mathbf{k}))$  which shows that any structure beyond the free-electron result that arises from a given region of  $k$  space will be summed over symmetrically related equivalent regions in the Brillouin zone (BZ).

<sup>12</sup>These are given in Ref. 7. Note, however, that they are "folded" in the sense discussed above (Ref. 9), since Fermi-surface dimensions were used in an analysis using a  $4 \times 4$  secular equation.

<sup>13</sup>H. Jones, *Proc. Phys. Soc.* 49, 250 (1937); M. A. E. Nutkins, *Proc. Phys. Soc. B* 69, 619 (1956).

<sup>14</sup>Though the sign of  $u_1$  is unimportant in what follows, the sign of  $u_2$  does have an influence on the ordering of levels. Again since we are illustrating a method with an example, we will choose  $u_2 > 0$  (as in aluminum). The case for  $u_2 < 0$  requires only minor modifications throughout.

<sup>15</sup>By geometrical arguments of equal simplicity we can calculate the first and fourth zone areas for free-electron energies slightly below or slightly in excess of  $e = \frac{5}{4}$ . Since  $(dS_3/de)_{e=5/4}$  can also be obtained we can determine with useful precision  $S_1$ ,  $S_2$  and  $S_3$  at the actual free-electron Fermi energy.

<sup>16</sup>Note that since the Fermi surface is largely free-electron-like away from these singular points, and the character of these points is identical to the points associated with  $L$  and  $X$  (they are all ordinary critical points), then with reasonable accuracy we may use the form of (15) as a basis for extending  $\delta g(e)$  away from the cusp itself.

<sup>17</sup>C. Herring, *Phys. Rev.* 52, 365 (1937).

<sup>18</sup>W. A. Harrison, *Phys. Rev.* 118, 1182 (1960).

<sup>19</sup>Aside from ensuring an ordering of bands that correctly leads to periodicity in reciprocal space, the assignment of the band index is conventionally effected in

such a way that  $\mathcal{E}_n(\vec{k}) \leq \mathcal{E}_m(\vec{k})$  implies  $n \leq m$ . This then guarantees that the surfaces of constant energy (branch  $m$  of which is defined by the solutions for  $\vec{k}$  (if they exist) of  $\mathcal{E}_m(\vec{k}) = \mathcal{E}$  will be continuous. Simple but crude estimates of the corresponding singular contributions to  $g(e)$  can be obtained using the methods of Ref. 5, but their overall scale is best determined numerically.

- <sup>20</sup>G. Gilat and L. P. Raubenheimer, Phys. Rev. 144, 390 (1966).
- <sup>21</sup>An accurate application of the Gilat-Raubenheimer technique to pseudopotential interpolated bands as calculated by Snow [Phys. Rev. 158, 683 (1967)] has been given by J. F. Janak and A. R. Williams [IBM Report RC 2411 (No. 11718), 1969 (unpublished)]. The results show most of the representative features of Fig. 8 although they are not identified in the manner described here.
- <sup>22</sup>L. Smrčka, Czech. J. Phys. B 20, 291 (1970).
- <sup>23</sup>R. Y. Koyama and N. V. Smith, Phys. Rev. B 2, 3049 (1970). Notice that spurious fine structure can be introduced into  $g(e)$  by numerical procedures which do not accurately distinguish between band extrema (which lead to Van Hove cusps) and band crossing (which lead to weak structure).
- <sup>24</sup>G. A. Rooke, J. Phys. C. 1, 767 (1968).
- <sup>25</sup>V. Hoffstein and D. S. Boudreaux, Phys. Rev. B 2, 3013 (1970).
- <sup>26</sup>J. W. D. Connolly, Int. J. Quantum Chem. IIIS, 807 (1970).
- <sup>27</sup>R. A. Tawil and S. P. Singhal, Phys. Rev. B 11, 699 (1975).
- <sup>28</sup>S. P. Singhal and J. Callaway, Phys. Rev. B 16, 1744 (1977).
- <sup>29</sup>P. Leonard, J. Phys. F 8, 467 (1978).
- <sup>30</sup>H. Bross, J. Phys. F 8, 2631 (1978).
- <sup>31</sup>H. Neddermeyer, Z. Phys. 271, 329 (1974).
- <sup>32</sup>J. C. Fuggle, E. Kallne, L. M. Watson, and D. J. Fabian, Phys. Rev. B 16, 750 (1977). The data reported here (and in Ref. 31) contain, of course, transition matrix elements which possess an energy dependence of their own which must be separated out before a direct comparison with Fig. 8 can be made.
- <sup>33</sup>See, for example, G. D. Mahan, in *Vacuum Ultraviolet Radiation Physics* edited by E. E. Koch, R. Haensel, and C. Kunz (Pergamon/Vieweg, Braunschweig, 1976), p. 635 (and references contained therein), and also J. D. Dow, *ibid.*, p. 649 (and, for reasons of equity, references contained therein as well). It should be noted that the point being made here concerning the possible importance of single-particle structure is entirely independent of one's stance towards the many-body corrections.
- <sup>34</sup>In other words, any further energy dependence of the pseudopotential, not contained in  $m^*$ , is being neglected.
- <sup>35</sup>C. Friedli and N. W. Ashcroft, Phys. Rev. B 12, 5552 (1975).